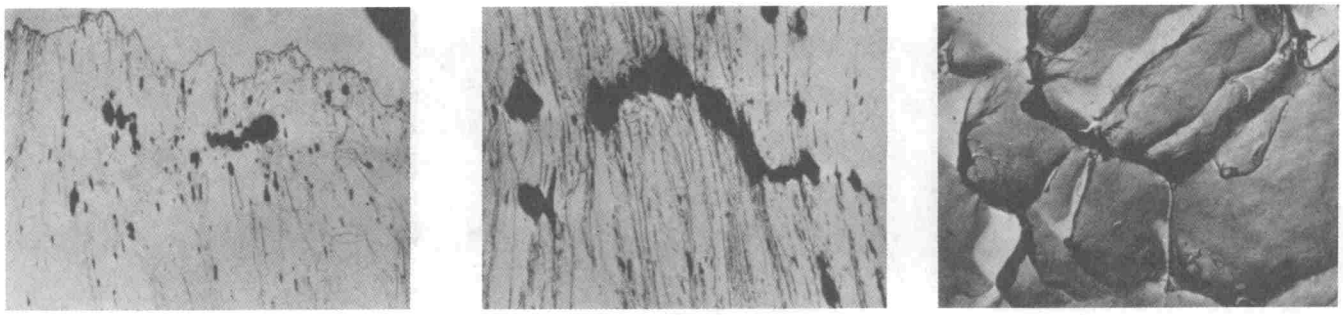

Fig. 3—Fracture in annealed 0.004 pct C material at atmospheric pressure. (*a*) and (*b*) magnification 106 times.

RESULTS

The presentation of the results will be divided into two categories consisting of 1) annealed 0.004 pct C and spheroidized materials and 2) annealed 0.40, 0.83, and 1.1 pct C materials.

1) Fracture in Annealed 0.004 pct C and Spheroidized Materials. a) *0.004 pct C Material.* Optical and electron fractographs of the 0.004 pct C material tested at atmospheric pressure are shown in Fig. 3. As can be seen in Figs. 3(*a*) and 3(*b*), the latter of which is a specimen strained to near fracture, the fracture mechanism involves the initiation, growth, and coalescence of massive voids. The major voids are limited to the center portion of the region of greatest necking where they grow and coalesce to form a major crack. In this region the electron fractograph, Fig. 3(*c*), shows equiaxed dimples corresponding to the "hills and valleys" seen in the fracture surface, Fig. 3(*a*).

The effects of pressure upon the fracture appearance are shown in Fig. 4. There is a progressive suppression of the void growth with increasing pressure as can be seen by comparing Fig. 3(*a*) with Fig. 4. At a pressure of 2.5 kbars, Fig. 4(*a*), only a few small elongated voids are in evidence. At 15.1 kbars, Fig. 4(*b*), there appears to be no discernible voids. There is a concomitant progressive change in the fracture profile from the "hill and valley" type at atmospheric pressure, Fig. 3(*a*), to primarily a series of shear steps at 2.5 kbars, Fig. 4(*a*), and finally to a flat planar shear type fracture at 15.1 kbars, Fig. 4(*b*). Due to the small cross sectional area at 15.1 kbars, it was not possible to obtain a reliable electron fractograph. However, from the appearance of the fracture surface shown in Fig. 4(*b*) and the results from the materials to be subsequently discussed, it is highly probable that the electron fractograph would be effectively featureless.

b) *Spheroidized Material.* The typical atmospheric pressure fracture appearance in the spheroidized materials is shown in Fig. 5. As can be seen, there are three distinct stages. Referring to Fig. 5(*b*), which is located just behind the fracture surface, the first stage is the fracture of the cementite particles. Second, voids form between the segments of the fractured particles. These voids grow laterally and longitudinally as the segments of the fractured particles move apart under the influence of the continued plastic strain of the ferrite matrix. Finally, as also shown in Fig. 5(*b*), the voids coalesce resulting in a

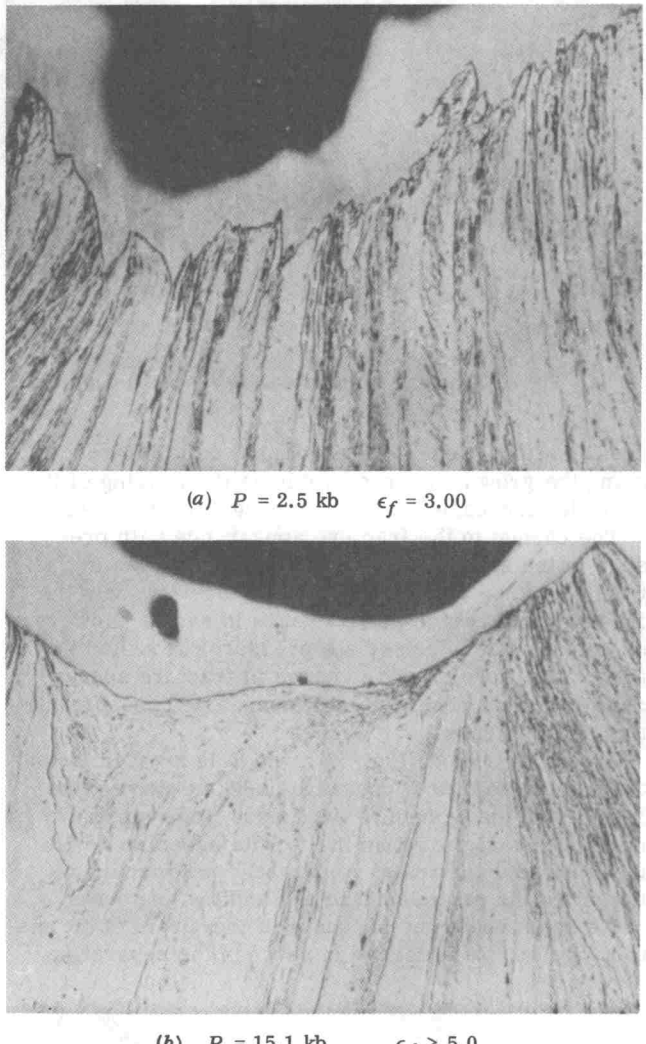

Fig. 4—Fracture in annealed 0.004 pct C material as function of pressure. Magnification 167 times.

major crack. These various steps in the fracture process are manifest in the fracture surface, Fig. 5(*a*), where one can see the remains of fractured cementite particles at the bottom of many "valleys". As would be expected, the electron fractograph, Fig. 5(*c*), consists of equiaxed dimples. The flat region (arrows) evident in some of the dimples in the fractograph corresponds to a fractured cementite particle.

The fracture appearance in the 0.40 and 0.83 pct C materials was effectively the same as that for the 1.1

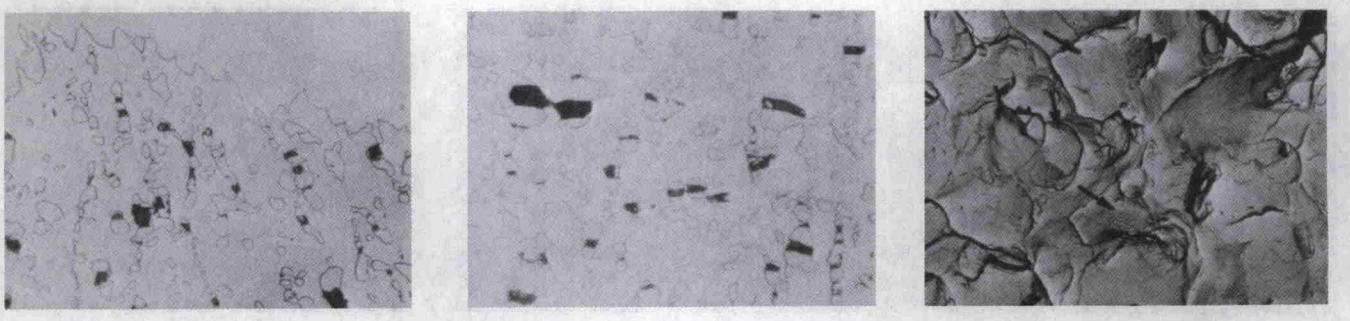

Fig. 5—Fracture in spheroidized 1.1 pct C material at atmospheric pressure. (*a*) and (*b*) magnification 530 times.

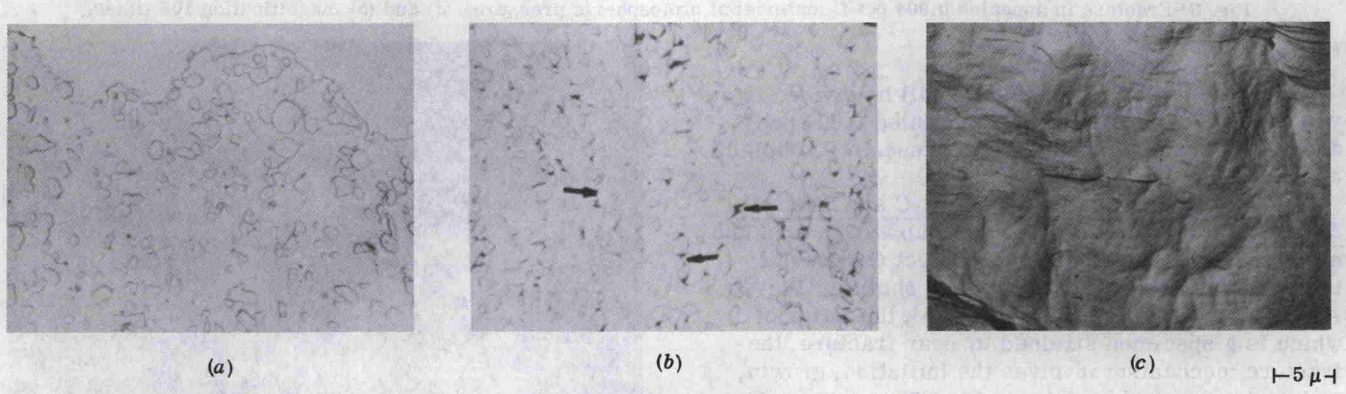

Fig. 6—Fracture in spheroidized 1.1 pct C material as function of pressure. (*a*) and (*b*) magnification 560 times.

pct C material described above, the only difference being the growth of larger voids as the spacing of the particles increased with decreasing carbon content.

The change in the fracture appearance with pressure in the spheroidized material can be seen in Fig. 6. It should be pointed out that, for brevity, only the fracture appearance at 21.3 kbars is shown. However, examination at intermediate pressures revealed that there was a progressive change in fracture appearance from that observed at atmospheric pressure to that at 21.3 kbars.

As can be seen in Fig. 6(*b*), which is an area behind the fracture surface, pressure does not prevent the fracture of the cementite particles. However, there is negligible void growth in the ferrite associated with the fractured particles. Apparently what occurs is that after the particles fracture and the segments move apart under the influence of the strain of the matrix, the ferrite is forced in between the separating segments. One can see in Fig. 6(*b*) the various stages of this process as depicted by the dark lines of varied widths connecting the two segments of fractured particles (arrows). Although it is difficult to match up the segments of a fractured particle once they are extensively separated, it appears that the ferrite surfaces between the segments are eventually forced together and rejoin.

The fracture surface, Fig. 6(*a*), shows no evidence of voids and the "hills and valleys" characteristic of fracture at atmospheric pressure. This is borne out by the electron fractograph, Fig. 6(*c*), which is effectively featureless and contains no indications of dimples or fractured cementite particles.

2) Fracture in Annealed 0.83, 0.40, and 1.1 pct C Materials. a) *Annealed 0.83 pct C Material.* The fracture appearance of this material at atmospheric pressure is shown in Fig. 7. The fracture surface, Fig. 7(*a*), consists of a series of approximately 45

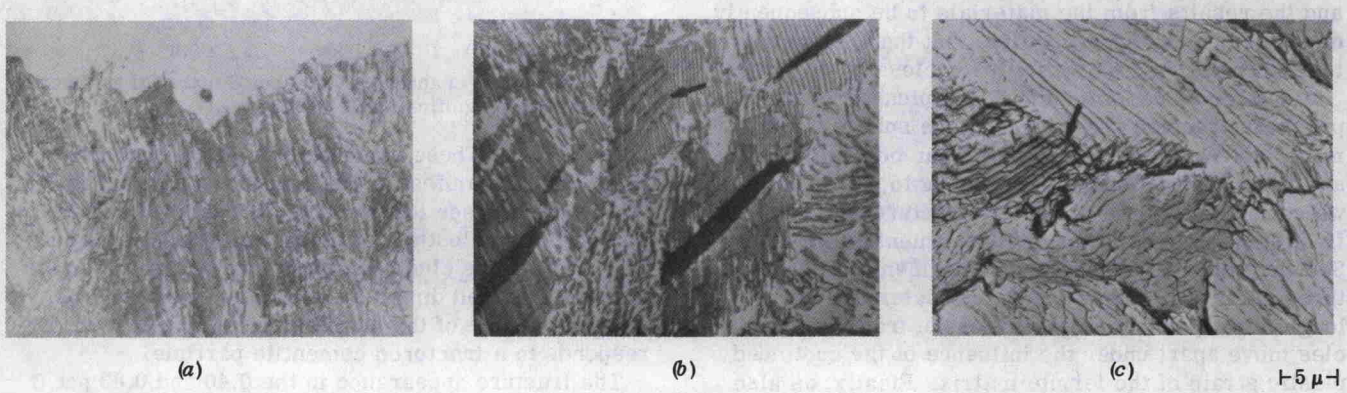

Fig. 7—Fracture in annealed 0.83 pct C material at atmospheric pressure. (*a*) and (*b*) magnification 530 times.